Supporting Information

Synthesis of thermoplastic elastomer from α-methylene-γ-butyrolactone for high temperature applications

*Friso G. Versteeg, Théophile Pelras, Giuseppe Portale and Francesco Picchioni**

Department of Chemical Engineering - Product Technology, University of Groningen, Nijenborgh 4, 9747 AG Groningen, The Netherlands.

Macromolecular Chemistry and New Polymeric Materials, Zernike Institute for Advanced Materials, University of Groningen, Nijenborgh 4, 9747 AG, The Netherlands.

Physical Chemistry of Polymeric and Nanostructured Materials, Zernike Institute for Advanced Materials, University of Groningen,9747 AG Groningen, The Netherlands.

Table of Contents:

Reversible addition-fragmentation chain-transfer polymerization mechanism

Initation:

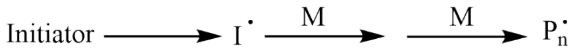

Pre-equilibrium:

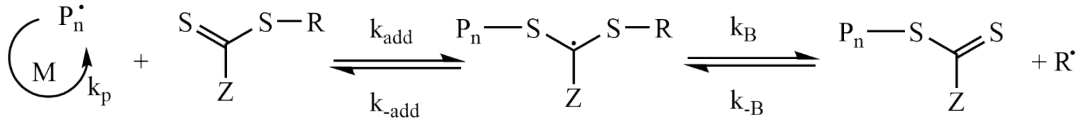

Reinitiation:

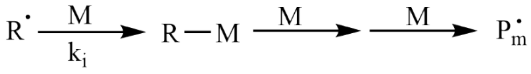

Main equilibrium:

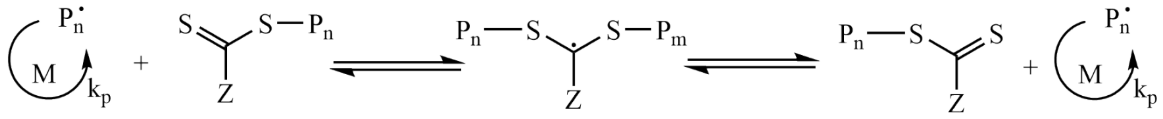

Termination:

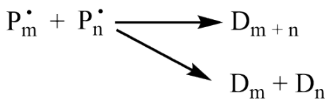

Fig. S1 Schematic drawing of the RAFT mechanism, redrawn from Perrier.[19]

The process, depicted in Fig. S1, starts with the decomposition of an initiator into a radical which will react with a monomer to form a propagating radical (i). After the initial propagation the polymeric radical reacts with the CTA. The selection of the a suitable CTA is crucial for the effectiveness of the polymerization. A fragmentation reaction may occur to form a new radical and a polymeric CTA (pre-equilibrium) (ii). The newly formed radical will undergo re-initiation with a monomer that will consecutively start a new polymeric chain. In the main equilibrium (iii) polymeric growth is occurring between the radical species that were not yet subjected to a termination reaction. The last step (iv) is the termination reaction where the growth of the polymeric chain is stopped and the remaining polymer molecule becomes a ‘dead polymer chain’. The term "dead polymer chain" refers to a polymer chain that has lost its ability to participate in further polymerization reactions. This loss occurs because the active radical site at the end of the chain has been terminated in a way that it can no longer react with monomers or other radicals.

Proton/Carbon nuclear magnetic resonance of CTA

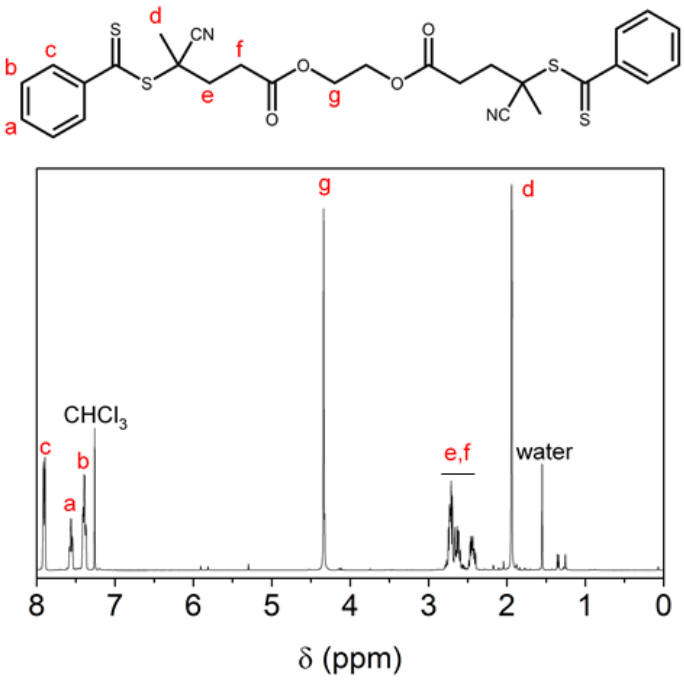

Fig. S2 ^{1}H-NMR spectra of the bisCTBPA in $CDCl_3$.

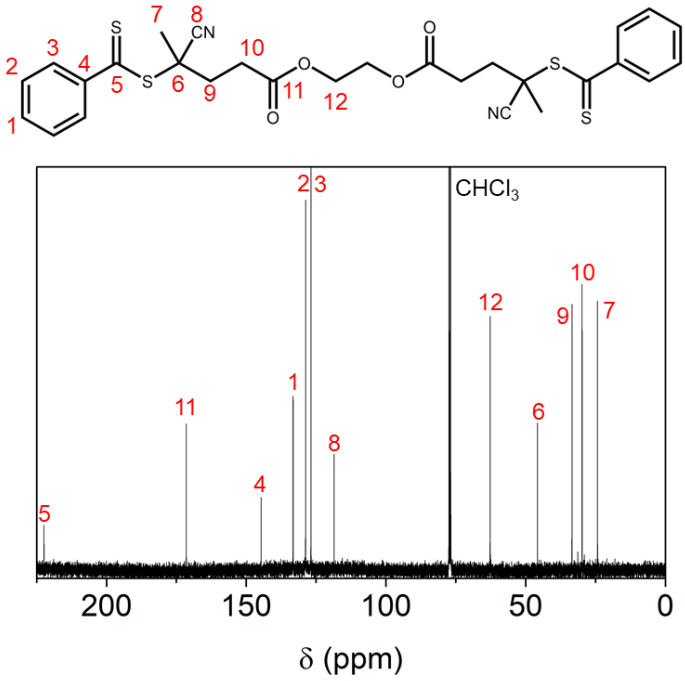

Fig. S3 ^{13}C-NMR spectra of the bisCTBPA in $CDCl_3$.

Homopolymerization of methyl methacrylate

bisCTBPA (1 eq, 19.9 mg, 34.0 µmol), MMA (102 eq, 346 mg, 3.46 mmol), AIBN (0.1 eq, 0.603 mg, 3.67 µmol; 112 µL of a stock solution containing 21.5 mg AIBN in 4.00 mL DMF) and DMF (1.5 mL) were charged into a round bottom flask equipped with a stirring egg. An aliquot was withdrawn for 1H NMR conversion analysis before the reaction mixture was deoxygenated via argon bubbling for 10 min and the flask immersed into a pre-heated oil bath at 70 °C. After 18 hours, the vessel was cooled down to room temperature and opened to air before withdrawal of an aliquot for 1H NMR conversion analysis. The polymer was precipitated into cold 6:1 *n*-hexane:ethanol, redissolved in minimal THF and further precipitated into pure n-hexane twice. The polymer was later redissolved in acetone, transferred to a clean vial and concentrated *in vaccuo*. Yield: 168 mg. 1H NMR: conversion = 79 %, DPNMR = 80, Mn NMR = 8 600. SEC: Mn SEC = 7 400, Đ = 1.16.

Table S1 Experimental result of homo RAFT polymerization of MMA

Sample	CTBPA:MMA	Conv (%)	DP_{NMR}	M_n (Da)[a]	M_n (Da)[b]	DP_{SEC}	PDI
PMMA	102	79	80	8600	7400	71	1.16

Scheme S1 homopolymerization of MMA.

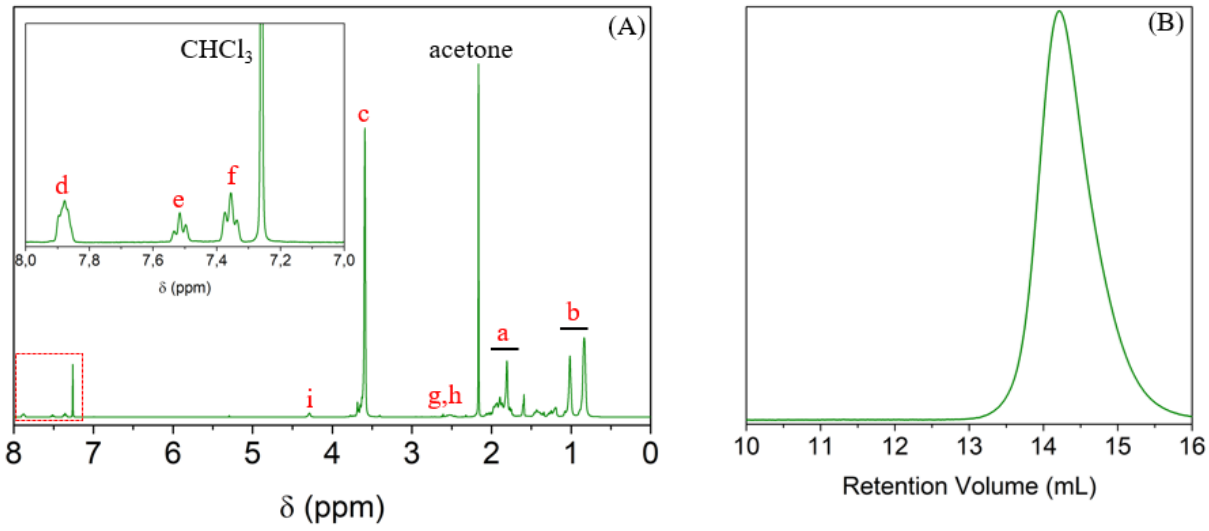

Fig. S4 ^{1}H-NMR spectra of the PMMA (A) in $CDCl_3$ and GPC results from PMMA (B).

Gel Permeation Chromatography

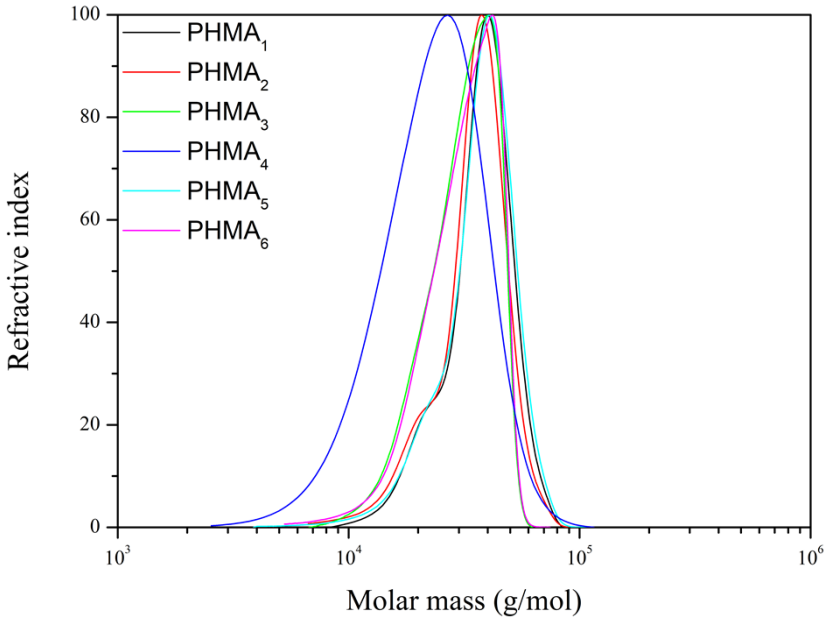

Fig. S5 GPC results of the $PHMA_x$ homopolymers.

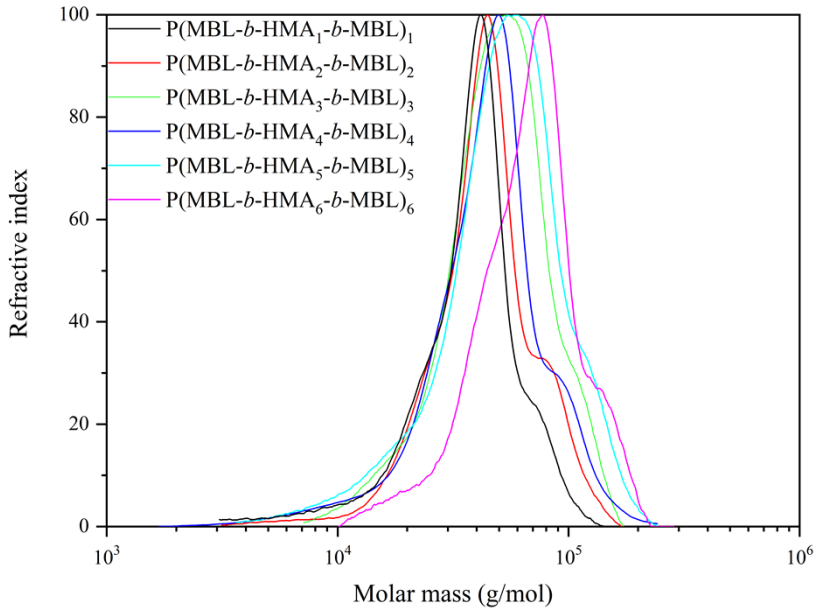

Fig. S6 GPC results of the P(MBL-*b*-HMA_x-*b*-MBL)$_x$ terblock copolymers.

Proton nuclear magnetic resonance of polymers

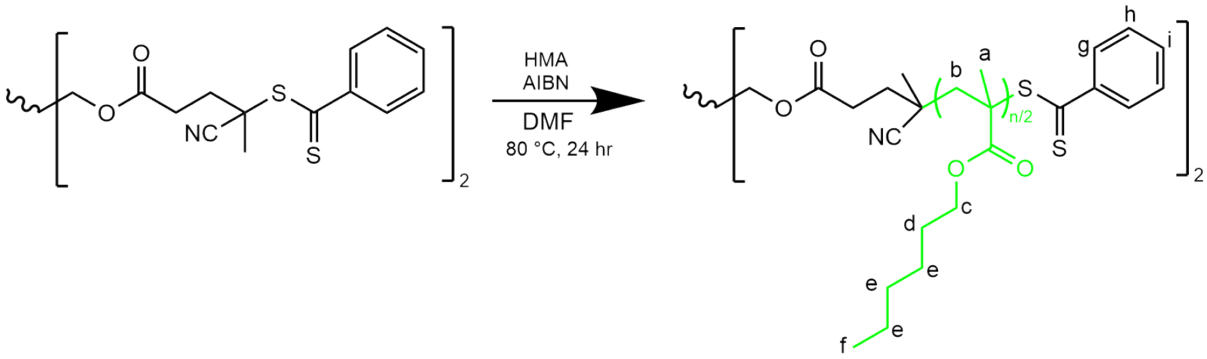

Scheme S2 homopolymerization of HMA.

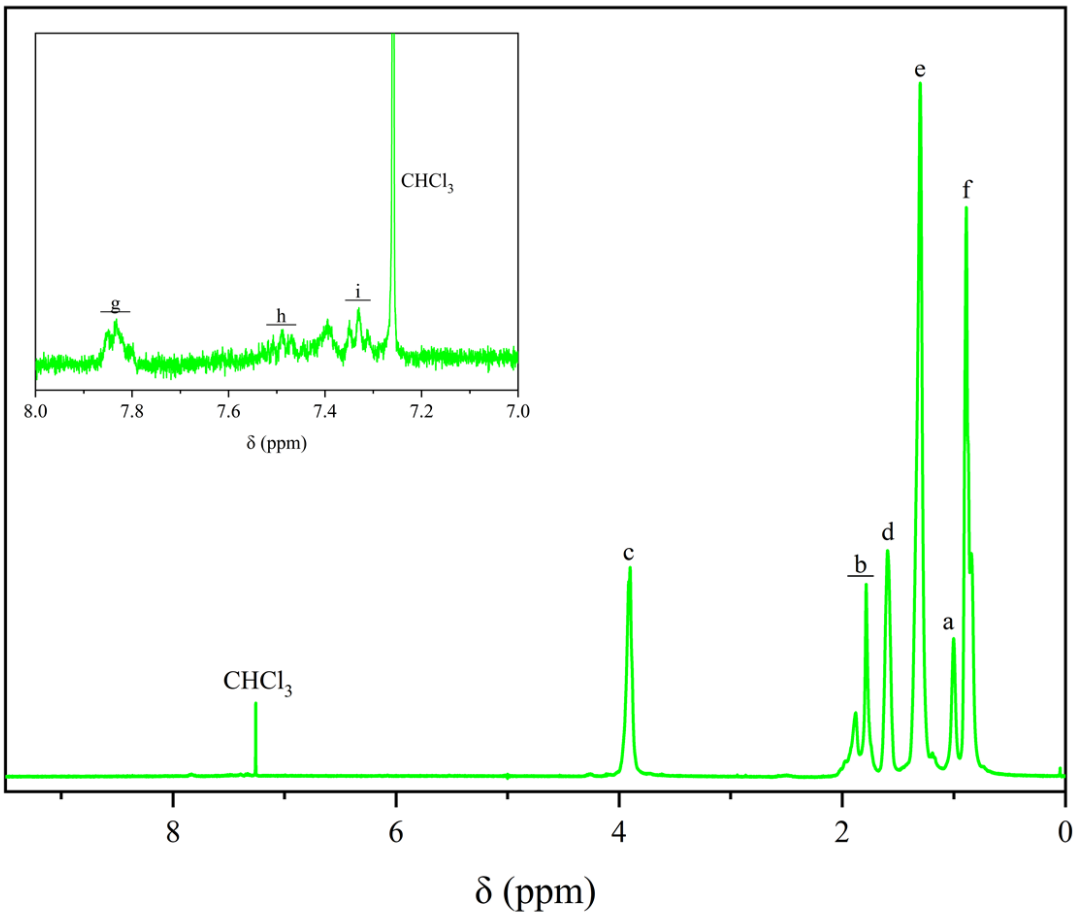

Fig. S7 ^{1}H-NMR spectra of (A) $PHMA_1$ in $CDCl_3$ and magnified between 7.0 and 8.0 ppm.

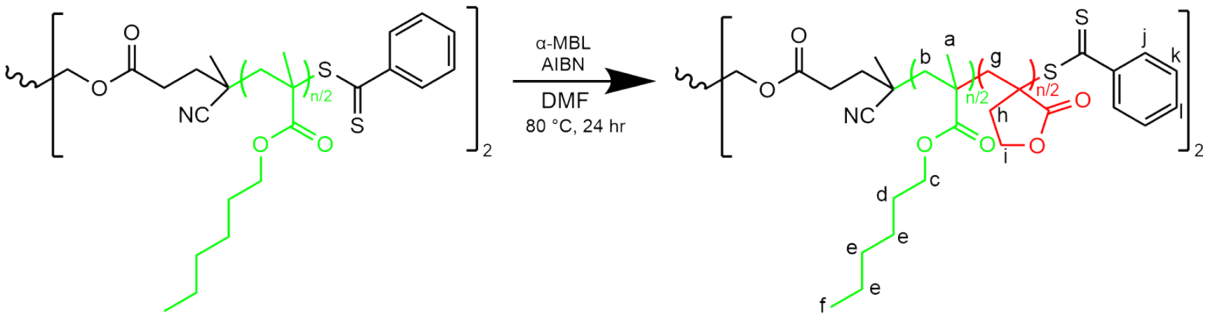

Scheme S3 Terblock copolymerization of P(MBL-HMA-MBL).

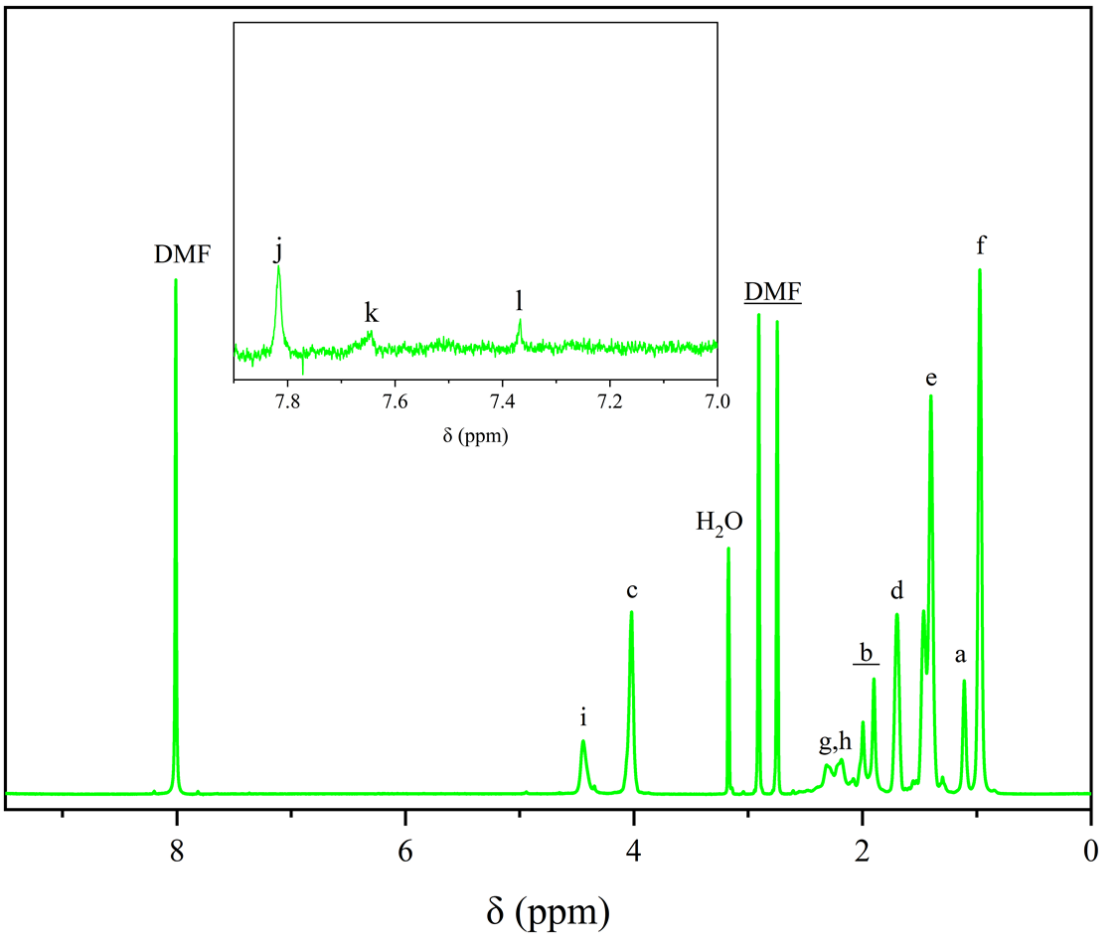

Fig. S8 ^{1}H-NMR spectra of (A) P(MBL-*b*-HMA$_2$-*b*-MBL)$_2$ in d$_7$-DMF and magnified between 7.0 and 8.0 ppm.

Fourier-transform infrared spectroscopy

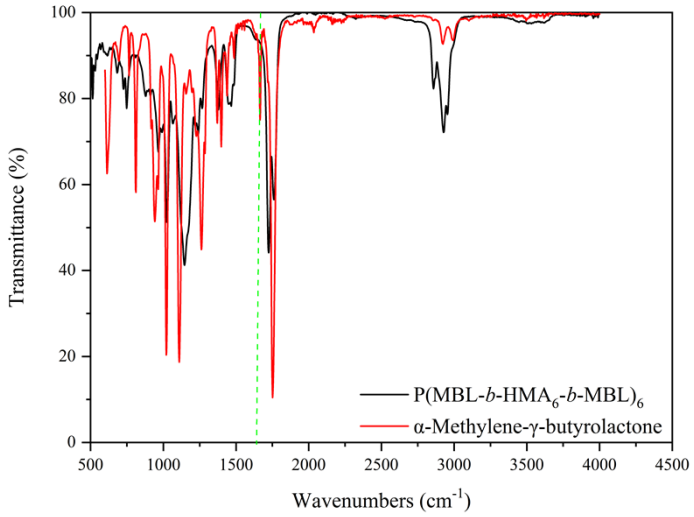

Fig. S9 IR spectrum of P(MBL-*b*-HMA_6-*b*-MBL)$_6$ and α-MBL

Differential Scanning Calorimetry

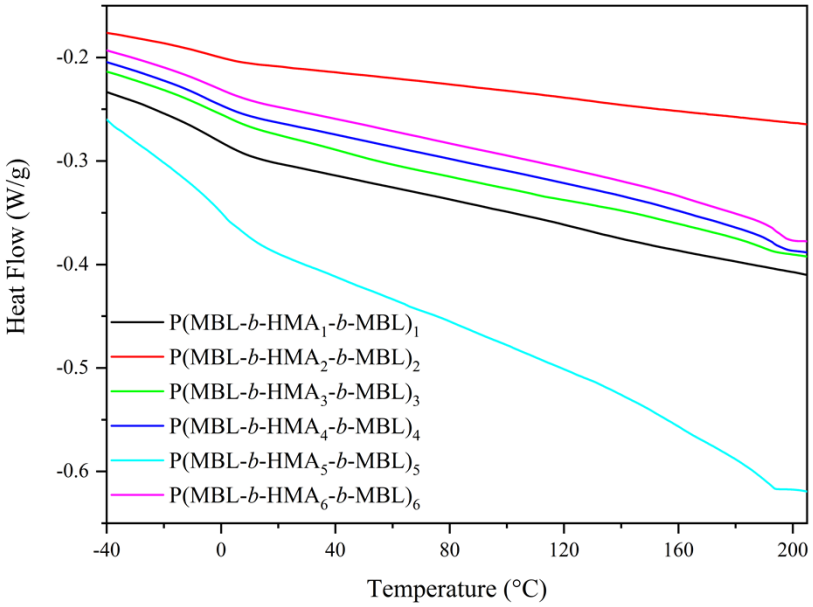

Fig. S10 DSC analysis of the P(MBL-*b*-$PHMA_x$-*b*-PMBL)$_x$ terblock copolymers.

Thermogravimetric analysis

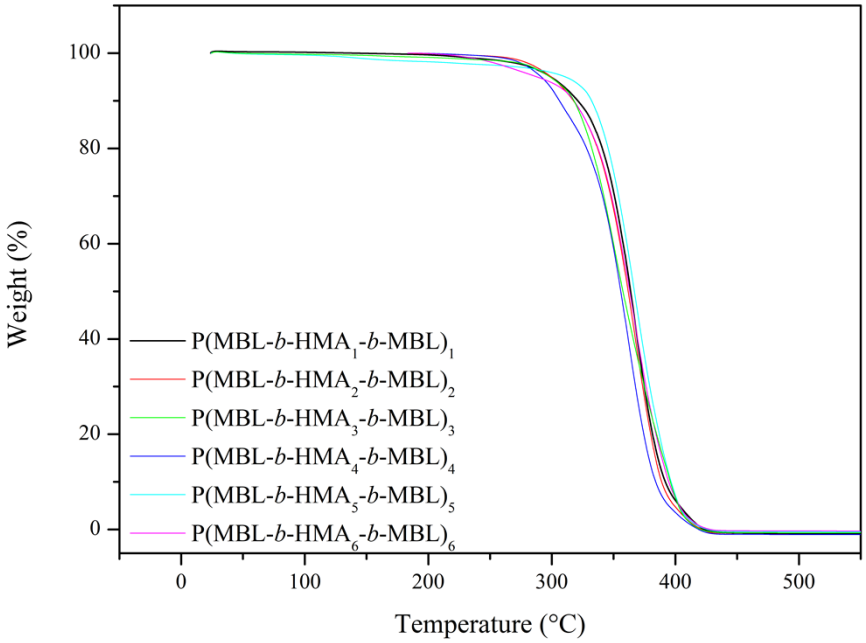

Fig. S11 Thermogravimetric decomposition results of the P(MBL-*b*-PHMA$_x$-*b*-PMBL)$_x$ terblock copolymers.

Table S2 Temperature onset of the triblock copolymers.

Blend	T_d (°C)[1]
P(MBL-HMA$_1$-MBL)$_1$	337
P(MBL-HMA$_2$-MBL)$_2$	333
P(MBL-HMA$_3$-MBL)$_3$	320
P(MBL-HMA$_4$-MBL)$_4$	327
P(MBL-HMA$_5$-MBL)$_5$	338
P(MBL-HMA$_6$-MBL)$_6$	332

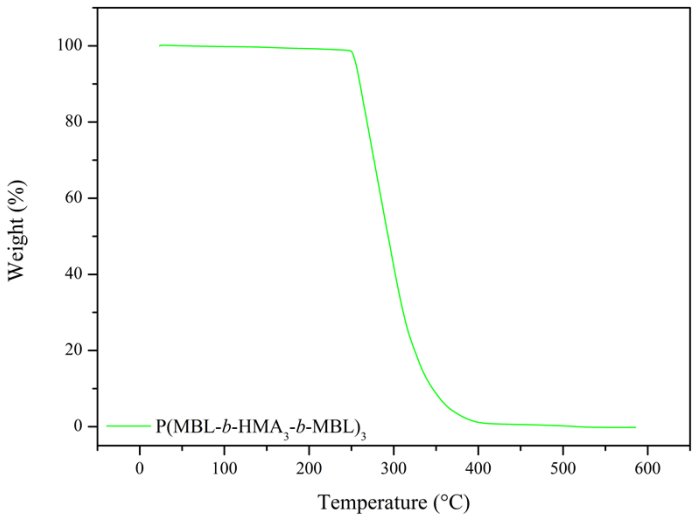

Fig. S12 Thermogravimetric combustion results of P(MBL-*b*-HMA$_3$-*b*-MBL)$_3$ terblock copolymer.

Rheology

Table S3 Power law fitting parameters of triblock copolymers at 110 °C.

Sample	*a*	*n*	R^2
P(MBL-HMA_1-MBL)$_1$	*103300*	*0.94*	*0.999*
P(MBL-HMA_2-MBL)$_2$	*235574*	*0.96*	*0.999*
P(MBL-HMA_3-MBL)$_3$	*309970*	*0.95*	*0.999*
P(MBL-HMA_4-MBL)$_4$	*1427908*	*0.95*	*0.999*
P(MBL-HMA_5-MBL)$_5$	*2016652*	*0.95*	*0.999*
P(MBL-HMA_6-MBL)$_6$	*11495891*	*0.95*	*0.999*

Table S4 Power law fitting parameters of triblock copolymers at 160 °C.

Sample	*a*	*n*	R^2
P(MBL-HMA_1-MBL)$_1$	*90508*	*0.94*	*0.999*
P(MBL-HMA_2-MBL)$_2$	*200872*	*0.96*	*0.999*
P(MBL-HMA_3-MBL)$_3$	*272299*	*0.94*	*0.999*
P(MBL-HMA_4-MBL)$_4$	*1115760*	*0.94*	*0.999*
P(MBL-HMA_5-MBL)$_5$	*1549947*	*0.95*	*0.999*
P(MBL-HMA_6-MBL)$_6$	*62541789*	*0.96*	*0.999*

Table S5 Power law fitting parameters of triblock copolymers at 200 °C.

Sample	*a*	*n*	R^2
P(MBL-HMA_1-MBL)$_1$	*62682*	*0.90*	*0.999*
P(MBL-HMA_2-MBL)$_2$	*157893*	*0.91*	*0.999*
P(MBL-HMA_3-MBL)$_3$	*204204*	*0.91*	*0.999*
P(MBL-HMA_4-MBL)$_4$	*499547*	*0.88*	*0.999*
P(MBL-HMA_5-MBL)$_5$	*658816*	*0.85*	*0.999*
P(MBL-HMA_6-MBL)$_6$	*1990121*	*0.72*	*0.999*

Table S6 Extrapolation of triblock copolymers at different frequencies at 110 °C.

Sample	*500 rad/s*	*1000 rad/s*	*10000 rad/s*
P(MBL-*b*-HMA_1-*b*-MBL)$_1$	300	156	18
P(MBL-*b*-HMA_2-*b*-MBL)$_2$	604	311	34
P(MBL-*b*-HMA_3-*b*-MBL)$_3$	846	438	49
P(MBL-*b*-HMA_4-*b*-MBL)$_4$	3897	2017	226
P(MBL-*b*-HMA_5-*b*-MBL)$_5$	5503	2849	320
P(MBL-*b*-HMA_6-*b*-MBL)$_6$	31370	16238	1822

Table S7 Extrapolation of triblock copolymers at different frequencies at 160 °C.

Sample	*500 rad/s*	*1000 rad/s*	*10000 rad/s*
P(MBL-*b*-HMA_1-*b*-MBL)$_1$	263	137	16
P(MBL-*b*-HMA_2-*b*-MBL)$_2$	583	304	35
P(MBL-*b*-HMA_3-*b*-MBL)$_3$	791	412	47
P(MBL-*b*-HMA_4-*b*-MBL)$_4$	2861	1471	161
P(MBL-*b*-HMA_5-*b*-MBL)$_5$	4230	2189	246
P(MBL-*b*-HMA_6-*b*-MBL)$_6$	160383	82446	9040

Table S8 Extrapolation of triblock copolymers at different frequencies at 200 °C.

Sample	*500 rad/s*	*1000 rad/s*	*10000 rad/s*
P(MBL-*b*-HMA$_1$-*b*-MBL)$_1$	233	125	16
P(MBL-*b*-HMA$_2$-*b*-MBL)$_2$	552	294	36
P(MBL-*b*-HMA$_3$-*b*-MBL)$_3$	714	380	47
P(MBL-*b*-HMA$_4$-*b*-MBL)$_4$	2106	1144	151
P(MBL-*b*-HMA$_5$-*b*-MBL)$_5$	3347	1857	262
P(MBL-*b*-HMA$_6$-*b*-MBL)$_6$	22679	13768	2623

Tensile Tests

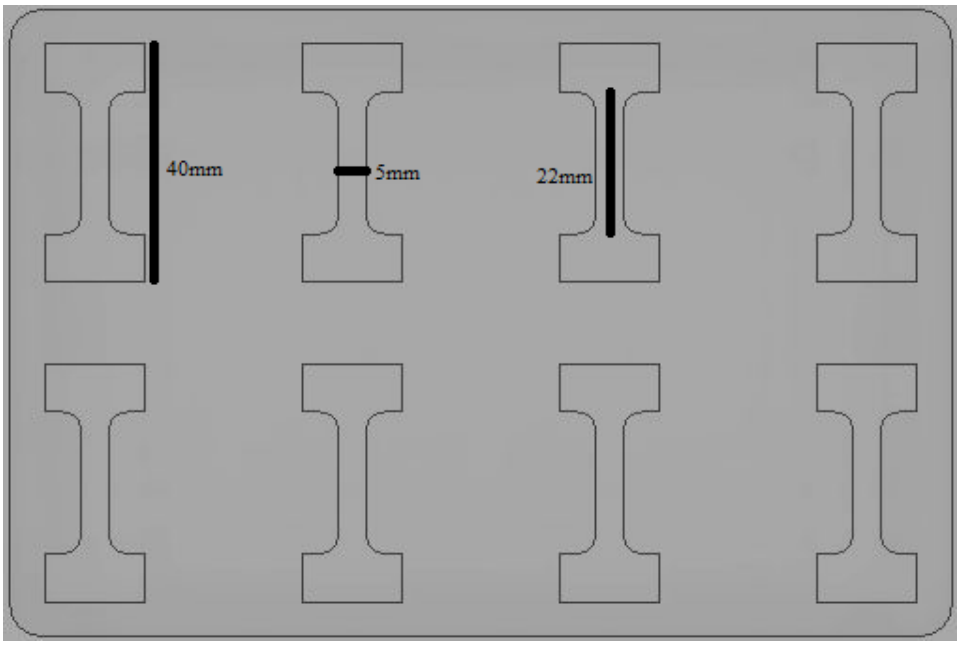

Fig. S13 Dimensions of the dumbbell molds.